Simulation of the Ionization Cooling of Muons in Linear RF Systems[*]

G. Penn, J.S. Wurtele, Department of Physics, University of California, Berkeley;
Center for Beam Physics, Lawrence Berkeley National Labs, Berkeley, CA 94720

Abstract

Ionization cooling of muon beams is a crucial component of the proposed muon collider and neutrino factory. Current studies of cooling channels predominantly use simulations which track single particles, an often time consuming procedure. These simulation efforts are discussed and compared with analytic studies using equations for the beam moments in a linear channel. These dynamic equations, which are analogous to the Courant-Snyder description of quadrupole focussing, incorporate the basic aspects of ionization cooling: energy loss and scattering in material, acceleration by radio frequency (RF) cavities, and focussing in solenoid magnets. This formalism can be used to study a wide range of cooling channels, and to evaluate the impact of engineering constraints on cooling channel performance.

1 INTRODUCTION

Interest in developing intense muon beams has been growing in recent years, both for a muon collider[1] and for a neutrino factory[2, 3]. The muon mass approaches the scale of the proton mass, without the internal structure. Furthermore, as a neutrino source, muon decays produce different pairs of neutrinos depending on the charge of the muons in the beam. Because of their μs half-life and the expense of producing muons, standard methods of beam preparation are not practical. Most schemes for producing muon beams use energetic protons incident on a target as a muon source, which results in a diffuse beam with a large energy spread requiring substantial beam cooling. The resulting six-dimensional phase space density must be increased by a factor of order 100 for a neutrino factory, and of order 10^6 for a muon collider.

Ionization cooling[4] is a promising alternative for producing a well-collimated beam. In ionization cooling, particles are slowed down by passing through material and re-accelerated with radio frequency (RF) cavities. This results in a reduction in transverse momentum, hindered by scattering events which increase the spread in particle angles. Such cooling channels have novel designs and concerns, and are currently simulated with single-particle tracking codes such as GEANT[5] and ICOOL[6].

To facilitate lattice design, it is desirable to have a rapid simulation tool with an accessible physical interpretation. Results for solenoid cooling channels are discussed which were obtained from beam moments equations[7] in the paraxial approximation, extending the Courant-Snyder[8] formalism for quadrupole lattices. These equations incorporate the main factors in ionization cooling: interactions with material, acceleration by RF cavities, and the possible accumulation of canonical angular momentum.

This set of equations has been incorporated into a version of the ICOOL simulation code for a rapid analysis of lattice properties and beam cooling performance. The results, applied to an engineered cooling channel design from the Fermilab feasibility study of a neutrino source[9], is compared with the ICOOL tracking code.

2 SINGLE-PARTICLE MOTION

We first consider single particle equations of motion in vacuum with magnetic fields only. The magnetic field inside of a cylindrically symmetric solenoid is given by $\vec{B} = \nabla \times [\mathcal{A}_\phi(r, z)\hat{e}_\phi]$. To lowest order in radius, $\mathcal{A}_\phi \simeq rB(z)/2$, where $B(z) \equiv B_z(r = 0, z)$. The constants of motion are total momentum and the canonical angular momentum, $L_{\text{canon}} = xP_y - yP_x + qr\mathcal{A}_\phi$. We can simplify these expressions if we consider a rotating coordinate frame (the Larmor frame), with $X_R = x \cos\varphi - y \sin\varphi$, $Y_R = x \sin\varphi + y \cos\varphi$, and

$$\varphi' = \frac{q\mathcal{A}_\phi}{P_z r} \simeq \frac{qB(z)}{2P_z} \equiv \kappa. \tag{1}$$

The linearized equations of motion in terms of these rotating coordinates reduce to $X_R'' = -\kappa^2 X_R$ and $Y_R'' = -\kappa^2 Y_R$; nonlinear terms only appear to third order in X_R and Y_R. In particular, coupling to longitudinal motion only appears in third order terms.

We can parametrize the solutions to the linearized equations in terms of a betatron function and phase by $X_R = A_1 \sqrt{\beta_p} \cos(\Phi - \Phi_1)$ and $Y_R = A_2 \sqrt{\beta_p} \cos(\Phi - \Phi_2)$. To this order, there are two additional constants of the motion, the transverse amplitudes A_1 and A_2 which correspond to the Courant-Snyder invariants. The betatron function must then satisfy $\Phi' = 1/\beta_p$ and

$$2\beta_p\beta_p'' - (\beta_p')^2 + 4\beta_p^2\kappa^2 - 4 = 0, \tag{2}$$

where $\kappa^2(z)$ is the linearized focussing term. In contrast with quadrupoles, the focussing strength is positive in both transverse directions, and increases as the magnetic field squared. The transverse amplitudes are determined from

$$A_1^2 = \frac{X_R^2}{\beta_p} + \beta_p \left(X_R' + \frac{\alpha_p}{\beta_p} X_R \right)^2, \tag{3}$$

where $\alpha_p = -\beta_p'/2$, and similarly for A_2.

Note that the focussing resembles that of a quadrupole lattice only in the rotating coordinate frame. In terms of these amplitudes, the angular momentum is $L_{\text{canon}} \simeq P_z A_1 A_2 \sin(\Phi_2 - \Phi_1)$. The evolution of the longitudinal momentum is consistent with $P_z^2 \left[1 + (x')^2 + (y')^2\right] = P^2$.

3 MODEL PARTICLE DISTRIBUTION

Above we examined individual particle trajectories; now we consider a simplified distribution in transverse phase space, which must be treated as 4-dimensional because of the coupling between x and y co-ordinates. For a cylindrically symmetric beam, the distribution should in general be a function of the angular momentum L_{canon} and the combined amplitude $A_1^2 + A_2^2$. A convenient form is the linear combination

$$A_\perp^2 \equiv \sqrt{1 + \mathcal{L}^2}(A_1^2 + A_2^2) - 2\mathcal{L}\frac{L_{\mathrm{canon}}}{P_z}, \qquad (4)$$

where $\mathcal{L}$ is a dimensionless parameter related to the net canonical momentum of the beam. This expression incorporates canonical momentum while ensuring that $A_\perp^2$ is always positive. A Gaussian beam will then have a distribution function given by

$$F = \frac{NP_z^2}{4\pi^2 m^2 c^2 \epsilon_N^2} \exp\left(-\frac{P_z A_\perp^2}{2mc\epsilon_N}\right), \qquad (5)$$

where $\epsilon_N = (P_z/mc)\langle A_\perp^2 \rangle/4$ is the normalized transverse emittance, and is related to the determinant of the 4×4 covariance matrix.

Expanding this total amplitude yields

$$
\begin{aligned}
A_\perp^2 &= \frac{x^2 + y^2}{\beta_\perp} + \beta_\perp\left(x' + \frac{\alpha_\perp}{\beta_\perp}x - \frac{\beta_\perp\kappa - \mathcal{L}}{\beta_\perp}y\right)^2 \\
&\quad + \beta_\perp\left(y' + \frac{\alpha_\perp}{\beta_\perp}y + \frac{\beta_\perp\kappa - \mathcal{L}}{\beta_\perp}x\right)^2,
\end{aligned} \qquad (6)
$$

where $\beta_\perp = \beta_p\sqrt{1 + \mathcal{L}^2}$ and $\alpha_\perp = \alpha_p\sqrt{1 + \mathcal{L}^2}$. We will see below that $\mathcal{L} \simeq \langle L_{\mathrm{canon}} \rangle/2mc\epsilon_N$. The shape of the beam envelope is described by $\beta_\perp$, $\alpha_\perp$, and $\mathcal{L}$.

For the Gaussian beam distribution given by Eq. (5), the symmetric transverse moments matrix M, which is also the covariance matrix, is

$$
\frac{M}{mc\epsilon_N} = \begin{pmatrix}
\beta_\perp/\langle P_z\rangle & & & \\
-\alpha_\perp & \langle P_z\rangle\gamma_\perp & & \\
0 & \beta_\perp\kappa - \mathcal{L} & \beta_\perp/\langle P_z\rangle & \\
\mathcal{L} - \beta_\perp\kappa & 0 & -\alpha_\perp & \langle P_z\rangle\gamma_\perp
\end{pmatrix}
\qquad (7)
$$

where

$$\gamma_\perp \equiv \frac{1}{\beta_\perp}\left[1 + \alpha_\perp^2 + (\beta_\perp\kappa - \mathcal{L})^2\right], \qquad (8)$$

and ϵ_N is the normalized transverse emittance. Note that the expression for $\gamma_\perp$ is different from that for a quadrupole even when $\mathcal{L} = 0$, because the moments are not taken in the rotating frame. The determinant of M simplifies to $\det M = [\langle x^2\rangle\langle P_x^2\rangle - \langle xP_x\rangle^2 - \langle xP_y\rangle^2]^2$, and the emittance satisfies $\det M = m^4 c^4 \epsilon_N^4$. The net canonical angular momentum is $\langle L_{\mathrm{canon}}\rangle \simeq 2mc\epsilon_N\mathcal{L}$.

In a vacuum with only magnetic fields, the parameters $\mathcal{L}$ and ϵ_N are constant, $\beta_\perp' = -2\alpha_\perp$, and

$$2\beta_\perp\beta_\perp'' - (\beta_\perp')^2 + 4\beta_\perp^2\kappa^2 - 4(1 + \mathcal{L}^2) = 0, \qquad (9)$$

which differs from the single particle case only through the term $1 + \mathcal{L}^2$. The resulting increase of $\beta_\perp$ with $\mathcal{L}$ reflects the fact that beams with canonical angular momentum have a larger spot size for the same emittance.

4 TRANSVERSE BEAM MOMENTS EQUATIONS

The evolution of an especially simple beam distribution was considered above; this example provides a model for analysing more general beams, as well as for parametrizing simulation results. The moments matrix M for any cylindrically symmetric beam has four independent terms, and can always be expressed in the form of Eq. (7) by a suitable choice of ϵ_N, $\beta_\perp$, $\alpha_\perp$, and $\mathcal{L}$. In addition, the average value of P_z is used; for example, we define the average linear focussing force to be

$$\kappa \equiv \frac{qB_z(r = 0, z)}{2\langle P_z\rangle} \simeq 0.15\frac{B[\mathrm{T}]}{P_z[\mathrm{GeV/c}]}\mathrm{m}^{-1}. \qquad (10)$$

The equations of motion for the beam envelope parameters, now redefined in terms of the lowest-order beam moments, can be derived by first neglecting multiple scattering and straggling, and assuming purely deterministic motion. Then an individual particle satisfies $x' = P_x/P_z$, $y' = P_y/P_z$, and

$$v_z\frac{d\vec{P}}{dz} = \frac{d\vec{P}}{dt} = q(\vec{E} + \vec{v}\times\vec{B}) + \vec{v}\frac{dP}{ds}. \qquad (11)$$

Note that dP/ds, the momentum change caused by material, is here defined as a negative quantity.

The averaging over particles which is performed when taking moments can be interchanged with the derivative, so that for example $d\langle x^2\rangle/dz = \langle 2xP_x/P_z\rangle$. This yields coupled equations for the four beam envelope parameters. Moments such as $\langle xE_x\rangle$ are set to zero, but they could be evaluated by a rudimentary space-charge model.

First, we add the effect of multiple scatter to this formalism. The spread in angles caused by multiple scatter is

$$\mathcal{S} \equiv \frac{d}{ds}\langle x'^2\rangle \simeq \left(\frac{13.6\ \mathrm{MeV}}{Pv}\right)^2\frac{1}{L_R}, \qquad (12)$$

using a Gaussian fit to the Moliere model of multiple scatter. Multiple scatter adds a quantity $P_z P\mathcal{S}$ to the rate of change in $\langle P_x^2\rangle$ and $\langle P_y^2\rangle$, leaving other derivatives unchanged.

In the limit where transverse fields are linear with radius and coupling to longitudinal motion is weak, the dynamic equations for the beam envelope are:

$$
\begin{aligned}
\epsilon_N' &= \beta_\perp\frac{P\mathcal{S}}{2mc} + \epsilon_N\frac{1}{P_z}\frac{dP}{ds}, \\
\beta_\perp' &= -2\alpha_\perp + \beta_\perp\frac{qE_z}{v_zP_z} - \frac{\beta_\perp^2}{\epsilon_N}\frac{P\mathcal{S}}{2mc} \\
&\quad - \frac{mc}{P_z}\beta_\perp\epsilon_N(\beta_\perp\kappa - \mathcal{L})\frac{qB'}{P_z},
\end{aligned}
$$

$$\alpha_\perp' = -\gamma_\perp + 2\kappa(\beta_\perp\kappa - \mathcal{L}) - \frac{\alpha_\perp\beta_\perp}{\epsilon_N}\frac{P\mathcal{S}}{2mc},$$

$$\mathcal{L}' = -\beta_\perp\kappa\frac{1}{P_z}\frac{dP}{ds} - \frac{\mathcal{L}\beta_\perp}{\epsilon_N}\frac{P\mathcal{S}}{2mc},$$

$$\langle P_z\rangle' = \frac{qE_z}{v_z} + \frac{dP}{ds} - mc\epsilon_N(\beta_\perp\kappa - \mathcal{L})\frac{qB'}{P_z}. \quad (13)$$

The longitudinal emittance tends to grow from a variety of effects including nonlinearities in the RF bucket, Landau straggling in material, and the differential rate of energy loss in material (slower particles tend to lose more energy in the relevant energy range). For a well-bunched beam having a large longitudinal emittance, with typical values being $10 - 30$ mm, the dominant effect is the slope of the energy loss curve, with the result that

$$\epsilon_L' \simeq \frac{1}{v}\frac{d}{dP}\left(v\frac{dP}{ds}\right)\epsilon_L. \quad (14)$$

5 AMPLITUDE CORRELATIONS

For beams having a large transverse emittance, the relative longitudinal motion of a particle is strongly dependent on transverse amplitude. This results in a significant nonlinear correlation being required in order for the beam to be matched into a given RF bucket. This effect on the longitudinal dynamics can be considered without re-evaluating the transverse motion of the particles.

The average forward velocity of a particle over many betatron oscillations is

$$\bar{v}_z \simeq v\left[1 - \frac{1}{4}(A_1^2 + A_2^2)\bar{\gamma}_p + \frac{1}{2P_z}L_{\text{canon}}\bar{\kappa}\right]. \quad (15)$$

For the case where $\bar{\kappa} = 0$ and $\mathcal{L} = 0$, the required momentum distribution for a matched beam can be described in terms of a single correlation parameter C_P as

$$P \simeq P_0\left(1 + C_P A_\perp^2\right) + \delta P \quad (16)$$

where P_0 is the nominal momentum and δP is a stochastic term. The matching condition is

$$C_P \simeq \frac{1}{4}\bar{\gamma}_\perp\left(1 + \frac{P_0^2}{m^2c^2}\right); \quad (17)$$

here, $\bar{\gamma}_\perp$ is the average value of $\gamma_\perp$ along the cooling lattice. The importance of this correlation will be examined in the simulations.

6 FOFO LATTICE

The cooling lattice considered here uses a magnetic field configuration where the field on axis varies with longitudinal position roughly as a sinusoid. This is here referred to as a FOFO ("focussing-focussing") lattice[10]. The properties of a FOFO lattice can be expressed in terms of the cell length and the distance of the beam momentum from the resonant momentum. The magnetic field on axis for the idealized lattice is $B_z(z) = B_{\max}\sin(2\pi z/L)$. There is a resonance at the critical momentum

$$P_{\text{cr}}[\text{GeV/c}] \simeq B_{\max}[\text{T}]L[\text{m}]/48.0, \quad (18)$$

where there is a phase advance of π radians per half period. Here, we focus on the parameter range where the beam momentum is greater than P_{cr}. All lattice parameters are determined by P_z/P_{cr} and the periodicity L.

For beams with $P_z > P_{\text{cr}}$, a rough fit to the numerical solutions can be found, which are correct in the limit of large momentum and properly exhibit the resonant behavior. For large momentum, the matched beta function is roughly constant and is determined by the average along the axis of the square of the magnetic field. The beta function is then given by $\beta_\perp \simeq 0.197\, LP_z/P_{\text{cr}}$, and the phase advance per half period is $2.54\, P_{\text{cr}}/P_z$. A numerical fit for the phase advance per half period is, in radians,

$$\Phi \simeq \pi\frac{P_{\text{cr}}}{P_z}\left\{1 - 0.19\left[1 - \left(\frac{P_{\text{cr}}}{P_z}\right)^2\right]^{1/2}\right\}.$$

This has the correct resonance and in addition reduces to the appropriate limit for momentum. A good fit for the minimum and maximum of the beta function is

$$\beta_{\substack{\min\\\max}} \simeq 0.197\, L\frac{P_z}{P_{\text{cr}}}\left[1 - \left(\frac{P_{\text{cr}}}{P_z}\right)^2\right]^{\pm 1/2}. \quad (19)$$

The specific channel used is a version of the cooling channel used in the Fermilab feasibility study of a neutrino source. A sketch of the cooling channel geometry as incorporated in the simulation is shown in Figure 1. The magnetic field has a period of 2.2 m, and the peak magnetic field on axis is 3.4 T. The nominal beam momentum of 0.2 GeV/c corresponds to $P_{\text{cr}}/P_z \simeq 0.78$. Liquid hydrogen absorbers for ionization cooling are centered around the zeroes of the magnetic field, where the beta function has its minimum value of $\simeq 40$ cm. The absorbers are 12.6 cm long surrounded by 400 μm thick aluminum walls. The radius of the absorbers is taken to be 15 cm. The RF cavities, operating at 201.25 MHz, are composed of pairs of pillbox cavities 32.93 cm long, with 17 cm radius windows composed of 125 μm thick beryllium. To maintain the beam momentum, the RF cavities have a peak field of 15 MV/m and are tuned for a phase of 29.7 degrees.

The initial beam has a normalized transverse emittance of 0.015 π m rad, and longitudinal emittance 0.015 m. The initial RMS bunch length is 10.5 cm. The beam has a Gaussian distribution except for a correlation between momentum and transverse amplitude as described above, with $C_P \simeq 4.3$ m^{-1}. This correlation has the effect of raising the average momentum to 0.227 GeV/c.

7 SIMULATIONS WITH PHASE SPACE CUTS

The figure of merit used here for the cooling channel is the number of particles propagating within the 6D phase space
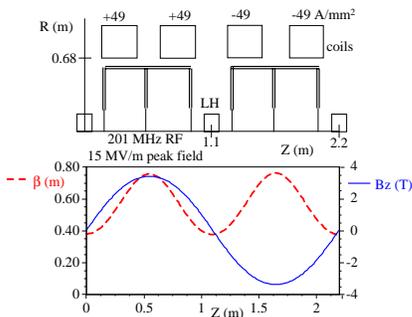
Figure 1: Sketch of a section of a FOFO cooling channel (above), with profiles of the beta function and magnetic field on axis (below).

acceptance of the subsequent acceleration stages. This consists of independent cuts on longitudinal and transverse amplitude, where transverse cut is taken to be $P_z A_\perp^2 /mc < 0.009375 \, \pi$ m rad, and the longitudinal phase space area is taken to be $0.15 \, \pi$ m. Recall that the typical value for transverse amplitude is $\langle P_z A_\perp^2 /mc \rangle \simeq 4\epsilon_N$. The fraction of the beam kept by each amplitude cut can be expressed in terms of the ratios $x_T \equiv P_z A_\perp^2 /2mc\epsilon_N$ and x_L, which is similarly defined for the longitudinal amplitude. The fraction of particles within the longitudinal cut is $f_L = 1 - \exp(-x_L)$, and for transverse cut is $f_T = 1 - (1 + x_T) \exp(-x_T)$. Values for the total fraction of the beam, $f_L f_T$, selected by the given phase space cuts are shown in Table 1 for several combinations of ϵ_N and ϵ_L. Note that the RMS emittance of the portion of the beam that survives the cuts is reduced from these values.

Table 1: Fraction of beam propagated within 6D phase space cuts.

ϵ_N (π **m rad**)	**fraction at** $\epsilon_L =$		
	0.060 **m**	0.030 **m**	0.015 **m**
0.015	0.0284	0.0365	0.0395
0.009	0.0689	0.0887	0.0959
0.004	0.233	0.300	0.325
0.002	0.485	0.623	0.675

Knowledge of the fraction of particles contained within transverse and longitudinal amplitude cuts can be used to model the RF bucket and radial apertures. Particles which are not contained by the RF system are accounted for by applying a longitudinal cut corresponding to the known size of the RF bucket. The longitudinal emittance of the beam before the cuts are applied is determined from Eq. (14). The scraping against radial apertures is determined by the beta function, the transverse emittance, and the maximum allowed radius, and is modelled by equating the maximum allowed radius to an effective cutoff in transverse amplitude. This cutoff is used to calculated both the fraction of particles which pass outside the aperture and the resulting

decrease in transverse emittance due to scraping. In this model, it is assumed that equivalent apertures will intersected by a given particle at a variety of betatron phases, so that particles at large angles are counted as lost even if the displacement is small.

The cooling channel performance is first shown for a matched beam that includes an energy-amplitude correlation. The simulation has been run for two lattices which differ by the removal of all radial apertures. Figure 3 shows the effect of the apertures to be small within the accelerator-defined acceptance region. If the apertures are removed, most of the particles with high transverse amplitude, which would have been scraped against the apertures, either are not sufficiently cooled to fit inside the transverse phase space cut by the end of the channel or are lost from other processes. There is good agreement with the moments equations, although the phase space density predicted by the moments equations is overly optimistic.
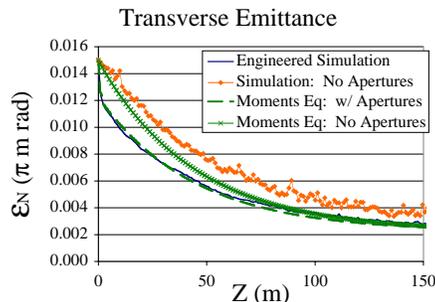
Figure 2: Normalized transverse emittance of beam. Comparison showing effect of radial apertures in simulations and from moments equations.
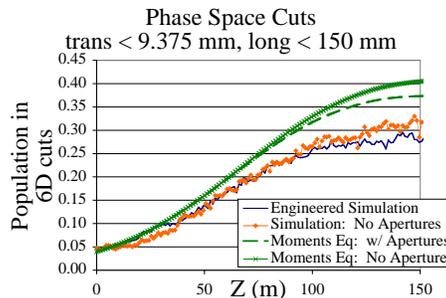
Figure 3: Fraction of initial beam within 6D phase space acceptance region. Comparison showing effect of radial apertures in simulations and from moments equations.

A similar comparison is made in Figures 4 – 6 for the cooling channel with radial apertures, shown for both the matched beam as above and a purely Gaussian beam without any energy-amplitude correlation. In this case a significant degradation of beam performance is shown to occur when the correlation is absent. For a beam with correlations, the moments equations are a closer fit to the simulation results. Further tailoring of the beam distribution

function for better longitudinal matching should yield results approaching the moments equations prediction; however, improvements beyond this value necessitate concrete changes in the channel geometry or in the fields. The beam without correlations is not well contained within the RF bucket, as indicated by the abrupt variations in the longitudinal emittance and greater particle losses. Note that inclusion of a single nonlinear correlation reduces by half the shortfall in performance between the purely Gaussian beam and the moments equations predictions.

Longitudinal Emittance

Figure 6: Longitudinal emittance of beam. Comparison showing effect of correlations in simulations and from moments equations.

Total Transmission
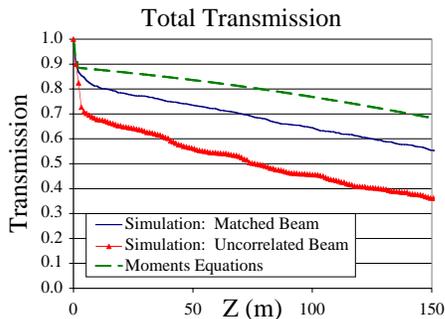
Figure 4: Total fraction of initial beam propagated through cooling channel. Comparison showing effect of correlations in simulations and from moments equations.

Phase Space Cuts
trans < 9.375 mm, long < 150 mm
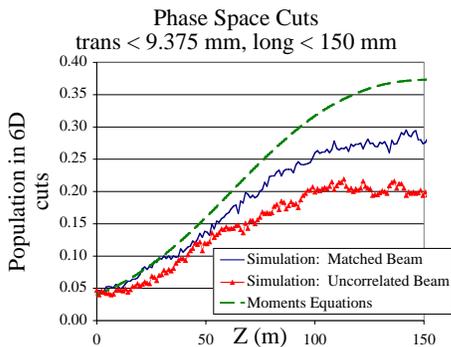
Figure 5: Fraction of initial beam within 6D phase space acceptance region. Comparison showing effect of correlations in simulations and from moments equations.

ments equations assume perfect matching of the beam in longitudinal phase space.

In addition, the longitudinal behavior of a beam has been evaluated in two limiting cases: where the beam is unbunched, in which case the average velocity as a function of energy and transverse amplitude is known; and for a well bunched beam, where correlations between energy and amplitude for a matched beam were found. The energy-amplitude correlation has been shown in the simulations to have a strong effect on achieved cooling performance. The apertures specified by the RF cavity design do not significantly impact the delivery of muons within the defined acceptance region in phase space, as demonstrated both in simulations and by using the beam moments equations extended to model beam scraping.

8 CONCLUSIONS

A paraxial theory has been developed for transverse beam moments in solenoidal fields, and applied towards a lattice designed for ionization cooling of muons. This theory is similar in form to the Courant-Snyder formalism for quadrupole focussing systems. The focussing properties are described in terms of the solenoid magnetic field on axis, while the transverse cooling depends on the material properties of the absorber placed in the beamline. This leads to a good prediction of lattice parameters required to propagate a beam and cooling performance, although the predicted results are optimistic because the transverse mo-

9 REFERENCES

[1] Charles M. Ankenbrandt et al. (Muon Collider Collaboration), Phys. Rev. ST Accel. Beams **2**, 081001 (1999).

[2] S. Geer, Phys. Rev. **D57**, 6989 (1998).

[3] Proceedings of the ICFA/ECFA Workshop "Neutrino Factories based on Muon Storage Rings", Lyon; to be published in Nucl. Instrum. Methods **A**.

[4] A.N. Skrinsky and V.V. Parkhomchuk, Sov. J. Part. Nucl. **12**, 223 (1981).

[5] GEANT4 Collaboration, CERN/LHCC 98-44, "GEANT4: An object-oriented toolkit for simulation in HEP"; see also http://wwwinfo.cern.ch/asd/geant4/geant4.html.

[6] R.C. Fernow, in Proceedings of the 1999 Particle Accelerator Conference, NY, p. 3020.

[7] G. Penn, J.S. Wurtele, Phys. Rev. Lett. **85**, 764 (2000).

[8] E.D. Courant and H.S. Synder, Ann. Phys. **3**, 1 (1958).

[9] T. Anderson et al., "A feasibility study of a neutrino source based on a muon storage ring", N. Holtkamp, D. Finley, eds., FNAL report FERMILAB-Pub-00/108-E June 2000.

[10] R.C. Fernow, Muon Collider Note 23 (unpublished). Available at http://www-mucool.fnal.gov/.